JEE Journal of Ecological Engineering

Journal of Ecological Engineering 2024, 25(6), 164–179
https://doi.org/10.12911/22998993/187148
ISSN 2299–8993, License CC-BY 4.0

Received: 2024.04.06
Accepted: 2024.04.26
Published: 2024.05.06

Synthesis of New Composite Adsorbents for Removing Heavy Metals and Dyes from Aqueous Solution

Layla Abdulkareem Mokif[1], Zahraa Hussein Obaid[1], Sarab A. Juda[1]

[1] Environmental Research and Studied Center, University of Babylon, Iraq
* Corresponding author's e-mail: laylaabdulkareem1986@gmail.com

ABSTRACT

In the current study, a novel composite (Fe_3O_4@MnO_2@Al_2O_3) was prepared to remove crystal violet dye and cadmium from aqueous solutions. The coprecipitation method was utilized to synthesize the composite. Batch studies were carried out using a contact period of 0.5–3 hours, an initial crystal violet and cadmium content of 50–200 mg/L, an agitation speed of 50–200 rpm, a pH of 4–12, and a composite dosage of 0.2–1.0 g per 50 mL of contaminated solution. The isotherm and kinetics models were formulated the experimental data. XRD, SEM-EDS, and FTIR analyses were utilized for composite characterization. The results revealed that the removal efficacy of crystal violet dye was 99.311% at 1 g of adsorbent, pH 12, 50 mg/L, 1 hour, and 200 rpm. The removal efficacy for cadmium (Cd) is 99.7296% at 1 g of sorbent mass at pH 6, 50 mg/L, 1 hour, and 200 rpm. The outcomes demonstrated that the Langmuir model could accurately depict the sorption of crystal violet dye onto the composite with R^2 (0.9882) and SSE (0.7084). On the basis of Freundlich, the capacity of the composite to reflect cadmium sorption was assessed by its highest R^2 (0.8947) and lowest SSE (8.5149). The pseudo-second-order model is a more realistic way to explain how cadmium and crystal violet dye sorb onto the composite. The results showed that the composite is effective in eliminating target pollutants, since cadmium has a maximum adsorption capacity of 48.5052 mg/g and crystal violet dye has a capacity of 40.9682 mg/g. Therefore, (Fe_3O_4@MnO_2@Al_2O_3) can be used as efficient sorbent for removing Cd and crystal violet dye from synthetic industrial wastewater.

Keywords: nanoparticles, Fe_3O_4, adsorption, cadmium, crystal violet dye, MnO_2, Al_2O_3, heavy metal.

INTRODUCTION

Sustainable water management is a persistent issue as a result of a growing number of factors, comprising the global population, the depletion of water supplies, and the rising demand for clean water, bioenergy, and food [1]. In response to the expansion of industry, a lot of home and industrial effluent is released into the water, which degrades water quality and causes pollution. Industrial wastewater has emerged as a widespread issue that worries people all over the world, since it exacerbates the global water crisis and poses a threat to human existence [2]. Wastewater must be treated before being released for final disposal, because it contains organic material, heavy metals, pathogenic microbes, and toxic compounds that pose a risk to environment and also to human health [3]. One of most distinguishable industries in the world, textile manufacturing and dyeing produces enormous amounts of wastewater (WW) containing refractory materials, like dyes and pigments [4]. The most significant origins of the industrial pollutants come from various industries, including the textile, food, cosmetic, leather, pharmaceutical, the varnish and paint, as well as paper and pulp industries. Textile, leather tanning, cosmetics, pigment, and many other sectors utilize dyes extensively to color products [5]. Large quantities of water are usually contaminated by synthetic colors employed in textile industries. Textile colors are usually released or thrown in the aquatic environment in the form of effluent due to no adherence to the secure fabric. As a result of this, the public health and environment are greatly harmed by the ongoing untreated outflow of the wastewater coming from many industries of textile. Both aquatic life and humans

are harmed by the chemical compounds found in contaminated water, which can be dissolved or solid in suspended form in an aqueous solution [6].

Textile dyes harm aquatic environments and may be hazardous to aquatic life, which could make their way into the food chain. A dye is possibly classified into eight different types based on its chemical composition, including azo dyes, and fourteen different categories based on its intended use, including reactive dyes, acid dyes, and so on. Due to the existence of chromophore and chromophore in the molecular structure, dyes exhibit chroma contamination [7]. The dyes include methylene blue (MB), Congo red (CR), methyl orange (MO), rhodamine B (RhB), methyl red, Disperse Violet 26, and crystal violet [5]. Dyes represent organic chemicals that are generated from a variety of industrial sources, comprising the textile, leather, paper, rubber, cosmetic, and even printing sectors. According to general estimates, dyes of about 0.7–1.6 million tons are yearly delivered to satisfy the requirements of modern demand, and about of 10–15% of such a volume is usually disposed of in the form of a wastewater, making it as a one of the major sources of water. The excessive exposure to dye can cause skin irritations, respiratory issues, and on rare occasions, it can even raise a person's risk of developing cancer [8]. More than 10,000 tons of synthetic dyes are exploited by textile industries each year out of the 7107 tons generated globally each year. In accordance with their origins, structures, and intended uses, the dyes are frequently divided into several groups. The industries of textile frequently employ azo, direct, acid, basic, reactive, mordant, dispersion, and sulfide dyes among these synthetic colors. Chemical, physical, and biological procedures are three categories into which the numerous dye removal methods are divided. While chemical modalities include ozonization, photo catalytic reaction, Fenton reagent, and biological modalities include aerobic degradations, anaerobic degradations, among others, physical methods include adsorption, ion exchanges, filtration/coagulation procedures, and others [9].

The most affordable and efficient approach of dye removal so far is the adsorption. Adsorbents like activated carbon are good at separating dyes from the industrial waste water effluents, but their somewhat high cost does not encourage their usage in large-scale applications. Experiments demonstrated that a variety of readily accessible non-traditional adsorbents can also be effectively utilized to remove dyes. As a result, research on finding effective and affordable adsorbents made from available resources is becoming more necessary for the removal of dyes [10].

Over time, both anthropogenic activities and natural occurrences emit toxins, particularly heavy metals, into the water. Adequate water treatment is required to reduce the negative impacts of the hazardous heavy metals in water [11]. Toxic metal pollution of the environment is a major cause for concern because these components have a significant impact on ecological systems. Toxic metals can accumulate at any point in the food chain and have a detrimental effect on all living things since they are incapable of being broken down by living things. Therefore, it is crucial to create the methods capable of removing dangerous heavy metals out of contaminated wastewaters [12]. Harmful effects associated with heavy metals on people include vomiting, diarrhea, typhoid, cancer, and severe liver and kidney damage [13]. Phytoremediation, ion exchange, precipitation, electrolysis, ultrafiltration, coagulation, flocculation, the reverse osmosis membrane, and the adsorption are among the most popular techniques used to remediate heavy metals out of polluted water [14]. The technique of adsorption is effective in removing the heavy metals out of the wastewater as a result of its accessibility, affordability, and environmentally friendly practices. The commercial adsorbents of high removal capacity and bioadsorbents are both exploited to remove the heavy metals from wastewater [15]. Metal oxides that are nanosized (such as zirconium oxides, aluminum oxides, iron oxides, and manganese oxides) have a high surface-to-bulk-atom ratio, a large surface area, and an extensive numbers of defect sites [16]. Using nanoparticles (NMs) to remove dyes seems to be a successful method [17]. Combination of their large surface areas, improved active sites in addition to functional groups existing on their surfaces, nanomaterials are considered as effective adsorbents for the removing of the heavy metals out of wastewater. Fe_3O_4 nanoparticles are frequently employed as an adsorbent to remove pollutants from water [18]. Fe_3O_4 nanoparticles have been synthesized using a number of different techniques, including coprecipitation [19–21] thermal decomposition, and green synthesis [22], sol gel, hydrothermal, electrochemical, and microemulsion. The most popular approach for preparing Fe_3O_4 nanoparticles is the coprecipitation method, since it is

quick and effective [23]. Due to readily available, inexpensive, and ecologically acceptable precursors, as well as simple experimental methods, co-precipitation represents by probably the most common approach to manufacture magnetic iron oxide nanoparticles. Chemical precipitation, gives reasonably reliable control on size and form of nanoparticles [24].

Co-precipitation of Fe^{3+} and Fe^{2+}, partial oxidation of Fe^{2+}, and partial reduction of Fe^{3+}, pursued by co-precipitation, are steps in the chemical precipitation process that produce magnetite [25]. Because Fe_3O_4 includes both ferric iron and ferrous at this ratio, the co-precipitation of Fe^{3+} and Fe^{2+} ions at a ratio of 1 to 2 in an alkaline medium can be considered as a one of the most well-liked, simple, and inexpensive routes of synthesis [26, 27]. Different morphologies of magnetic Fe_3O_4 NPs, including nanoparticles, nanocubes, octahedral, and rhombic dodecahedrons, have been developed through synthetic approaches [28]. Because of their superior mechanical and magnetic capabilities, nanomaterials, particularly metal oxides have been widely exploited as magnetic storage materials and catalysts throughout the past two decades. Because of their low cost, low toxicity, and strong magnetic characteristics, iron oxide nanoparticles (Fe_3O_4 NPs) represent the most well-known and widely used type of magnetite nanomaterials [29].

A number of their special qualities like superparamagnetism, low toxicity, and capacity to form bonds with the biological molecules, magnetite nanoparticles are well suited for medication delivery, diagnostic procedures, and treatment approaches. Fe_3O_4 nanoparticles are employed for the adsorption of many metals, including arsenic lead, and chromium. Additionally, the removal of dyes like methylene blue, methyl red, bromophenol blue, bromocresol green, and erichrome black-T is also accomplished using Fe_3O_4 nanoparticles [30]. Fe_3O_4 has the benefit of being the most straightforward to separate from solution after adsorption procedure. Since magnetite contains both ferrous and ferric iron, it is frequently called Iron II, III Oxide. In addition to increasing the lattice parameters and unit cell volumes, nanoscale magnetite (Fe_3O_4) has also unquestionably raised the effective area and surface area. Through the copolymer synthesis process, magnetite can enhance the electrical characteristics of a polymeric material. Therefore, a feasibility assessment for creating industries for the production of Fe_3O_4 is required, particularly in poor nations. In spite of their capacity for formation complexes with numerous ions of heavy metals like Cd, Zn, Cu, and Pb and their high chemical stability in both basic and acidic environments, manganese oxides are considered as excellent adsorbents [23, 31].

Various chemical substances, comprising endocrine disruptors, antimicrobial agents, and the pharmaceuticals, manganese oxide, are also regarded as favorable oxidants. Additionally, MnO_2 NPs have had their redox and sorption characteristics studied from a technical perspective for potential use in water oxidation catalysis or remediation strategies [32]. Aluminum oxide nanoparticles are a cheap surface, which has several features that cause it as an effective surface in the dye removal, because it possesses a large surface area, surface responsiveness, surface acidification, strong adsorption capacity, and many hydroxide groups [33]. The objectives of this study are: i) preparation of a new composite ($Fe_3O_4/MnO_2/Al_2O_3$) via co-precipitation method ii) investigation the efficiency of the prepared composite for the treatment of an aqueous solution contaminated with crystal violet dye and cadmium through batch experiments.

MARTIALS AND METHODS

Chemicals and contaminants

The chemicals used in this work were ($FeCl_2 \cdot 4H_2O$), aqueous ammonia (20%), hydrochloric acid (HCl 37%), aluminum oxide (Al_2O_3) and NaOH which are supplied from marked. The target contaminants used in this study were crystal violet dye ($Cl_{30}H_3N_{25}C$) and Cadmium (Cd). The stock solutions of crystal violet dye and Cadmium were prepared by dissolving 1 g of each contaminant per 1000 ml of distilled water (DW). Shimadzu UV-1900i UV visible spectrophotometer was used for measuring the concentration of the crystal violet dye at wavelength of 590 nm. Atomic absorption spectroscopy was used for estimating the concentration of cadmium.

Preparation of the composite ($Fe_3O_4@MnO_2@Al_2O_3$)

Nanoparticles of Fe_3O_4 were prepared by the coprecipitation method as stated in previous study [27]. For preparation of the Fe_3O_4 nanoparticles, a specific amount of $FeCl_2.4H_2O$ (1M) was dissolved in aqua DM. HCl (37%) was added to

the solution of $FeCl_2.4H_2O$ and stirred at room temperature then the pH adjustment until pH = 11 was achieved via adding aqueous ammonia (20%) and digested the mixture for (30) min at 70 °C until precipitate was yielded. The excessive molecules of the ammonia contained in the precipitate were then removed by washing it with aqua DM. After drying at 70 °C, the Fe_3O_4 nanoparticles were eventually obtained as a black powder. The synthesis methodology of MnO_2 was similar to that used in the literature reviewed [34]. After first dissolving potassium permanganate in distilled water, ethanol was added. The mixture was agitated until a precipitate of the manganese oxide (brownish-black) was obtained. The precipitate was washed with a distilled water and filtered with Whitman filter paper to remove the undesirable contaminants. The precipitate was then dried for 24 hours at 60 °C in a vacuum oven to eliminate any remaining moisture before use. The composite used in this study was prepared by mixing synthesized Fe_3O_4, MnO_2 and Al_2O_3, respectively, with a mixing ratio of (1:1:1). Figure 1 illustrates the synthesis process of the composite.

BATCH TESTS

The batch tests were accomplished at room temperature. In batch tests, the impact of various parameters was investigated, including contact time 0.5–3 h, initial concentration of cadmium and crystal violet dye 50–200 mg/L, pH 4–12, agitation speed of 50–200 rpm, and mass (dosage) of adsorbent of 0.2–1.0 g, contaminant solution volume of 50 ml. For the experiment, several flasks were filled with contaminated solution of 50 ml. The impact of different parameters was studied separately for two contaminants (crystal violet dye and Cd) in these batch experiments for detecting of optimum parameters. The pH of experiments was adjusted through NaOH and HCl (0.1 M). As soon as the equilibrium is approached, filter paper was used for the separation of adsorbent from contaminated solution. Eq. 1 is employed for measuring of the contaminants quantity (q_e) retained on composite adsorbent at the equilibrium condition. Eq. 2 may be used to estimate the percentage removal (R%) of contaminants [35]. All batch experiments were conducted separately for each contaminant.

$$q_e = \frac{(C_o - C_e)V}{m} \quad (1)$$

$$R(\%) = \frac{C_o - C_e}{C_o} \times 100 \quad (2)$$

MODELING OF SORPTION DATA

Sorption isotherm

Two models were used for expressing of sorption isotherm, including the Langmuir and Freundlich models. The Langmuir model is employed for estimating the maximum sorption capacity (q_{max}, mg/g) of produced sorbent and is expressed as follows:

$$q_e = \frac{q_{max} b C_e}{1 + b C_e} \quad (3)$$

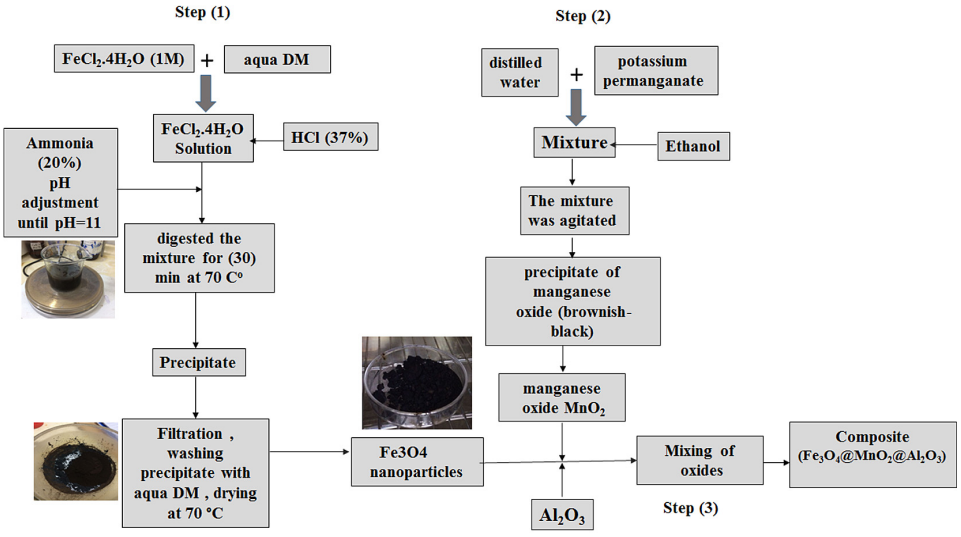

Figure 1. Synthesis process of composite adsorbent

where: b represents the sorbent particles - contaminant molecules affinity (L/mg).

The Freundlich model is applied for multilayer sorption onto nonhomogeneous surface and is expressed as follows:

$$q_e = K_f \, C_e^{\frac{1}{n}} \quad (4)$$

where: K_f represents the Freundlich constant and the factor 1/n (< 1) refers to intensity of sorption [36] Faddak farm, Kar-bala Governorate, Iraq proved that the sulfate (SO_4^{2-}).

Kinetic adsorption models

Two models were utilized for adsorption kinetic, which are presented in Eq's. 5, 6 and 7. These models were applied to a wide variety of adsorption systems, comprising heavy metals and pharmaceuticals as pollutants in addition to biomass and nanomaterials as adsorbents.

Pseudo-first order model: is simply a well-known formula used to express the solute sorption rate of [37]:

$$q_t = q_e(1 - \mathrm{e}^{-k_1 t}) \quad (5)$$

where: k_1 represents the rate constant (1/min), and the q_t and q_e (mg/g) are the quantity of solute retained on the adsorbent at time t and the equilibrium state, respectively.

Pseudo-second order model: The energy of sorption cannot change for each sorbent, where there is nonexistence of interaction condition between the sorbed chemicals, and only one layer of the considered solute can adhere to sorbent particles, according to this model. It is presented in Eq. 5 [38]:

$$q_t = \frac{k_2 q_e^2 t}{(1+k_2 q_e t)} \quad (6)$$

where: k_2 represents the rate constant corresponding to 2nd order model (g/mg min).

RESULTS AND DISCUSSION

Influence of contact time

In batch experiments, the time required to attain equilibrium condition is a critical step in determining the contaminants distributed throughout the adsorbent and solution phases. Figure 2 shows the change in crystal violet dye and cadmium (Cd) adsorption effectiveness over contact time up to 3 hours at an initial concentration (Co) of 50 mg/L, composite dosage of 0.5 g/50 mL, pH 7, and an agitation speed of 200 rpm. The crystal violet dye and Cd are removed highly at the starting instance of the test, and then the rate is possibly to be reduced after one hour as a result of the reduction in the vacant sites [39]. Throughout the first hour, the removal percentage grew exponentially with increasing contact time. However, at the saturation point, the adsorbent surface can only weakly hold the dye molecules [40]. As the adsorption time increased, the adsorption of Cd^{2+} by the adsorbent became more difficult due to the fact that the active sites had been fully occupied and also the positive charges of the ions in the

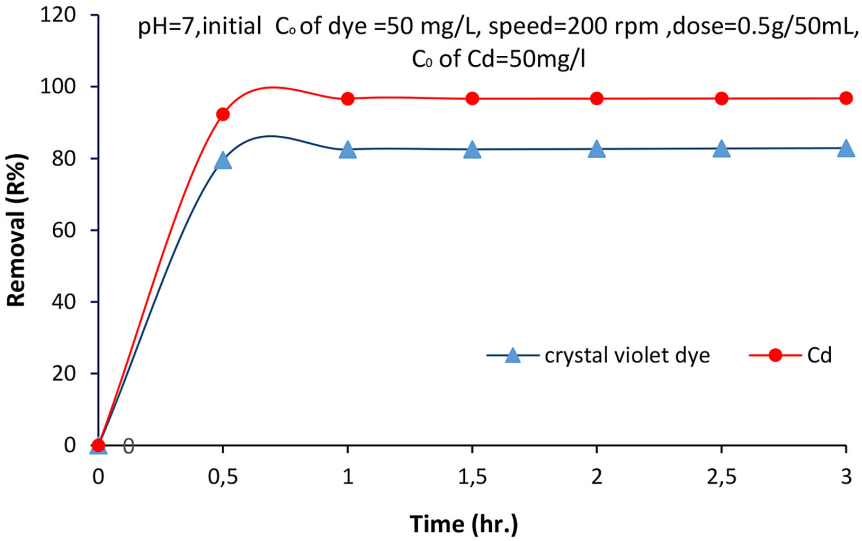

Figure 2. Effect of contact time on the manufactured composite adsorbent behavior used for removing dye and cadmium from contaminated aqueous solution

adsorbed metal resisted the metal ions existing in the water. In the end, this increases the adsorption rate till equilibrium state [41]. The outcomes reveal that the dye and Cd sorption efficacy were 82.51% and 96.65%, respectively at 1 h; nevertheless, there is no noticeable rise in the percentages of removal beyond this time until 3 h.

Influence of initial concentration

The initial concentration is a major variable in adsorption experiments, since it determines the adsorption rate. Figure 3 clarifies that the initial concentration has a distinguishable effect upon the removal effectiveness of Cd and crystal violet dye. These removal efficiencies were significantly lowered, from 82.52 to 50.5 for crystal violet dye and from 96.654% to 70.881% for Cd as a result of variation of Co from 50 to 200 mg/L, at 1 h, pH 7, a speed of 200 rpm, and composite dosage of 0.5 g/50 mL. At lower levels of the concentrations, it is expected that all contaminant molecules will come into contact with the accessible binding sites, which is certain to cause a significant increase in the effectiveness of sorption; however, an excessive amount of the contaminant molecules as a result of rise in concentration with specific grams of composite can cause a reduction in this efficiency [42, 43]. The quantity of dye molecules grew as the concentration gradient became steeper. This causes an increase in the driving force between the solid and liquid phases, which aids in overcoming the mass transfer resistance of dye molecules [44].

Influence of agitation speed

One important factor to consider in adsorption investigation is the agitation speed. The dispersion of pollutant molecules in the solution is one way it affects the formation of the external boundary layer [56]. Figure 4 exhibits the impact of agitation speed on removal efficacy of crystal violet dye and Cd. Increasing agitation speed led to improved contaminant removal efficiency. The rapid agitation speed promotes the pollutant's diffusion via composite, resulting in effective interactions between contaminants and adsorption sites. The outcomes demonstrated that a 200 rpm agitation speed was sufficient for maximum absorption of crystal violet dye and Cd, respectively, with no noticeable difference in removal rates after this number.

Influence of initial pH

The solution pH is generally affecting the negatively and positively charged composite surface molecules. Their charge is altered to be more positively or negatively charged through the process of proton gain or loss [45]. Degree of the ionization, and the dissociation of the functional groups are all influenced by the pH of the solution [44]. Figure 5 illustrates the effect of pH on the removal efficiency of the crystal violet dye and Cd

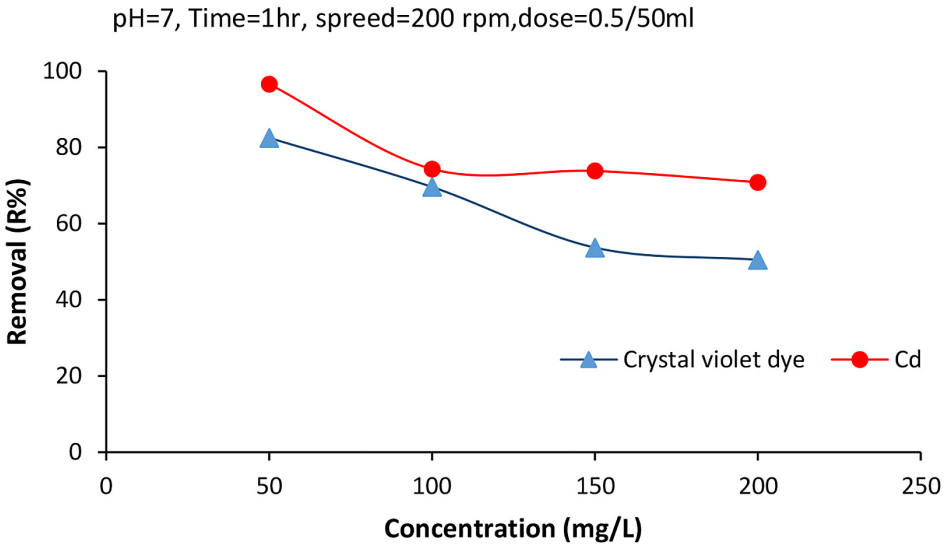

Figure 3. Effect of initial contaminants concentration on the manufactured composite adsorbent behavior used for removing dye and cadmium from contaminated aqueous solution

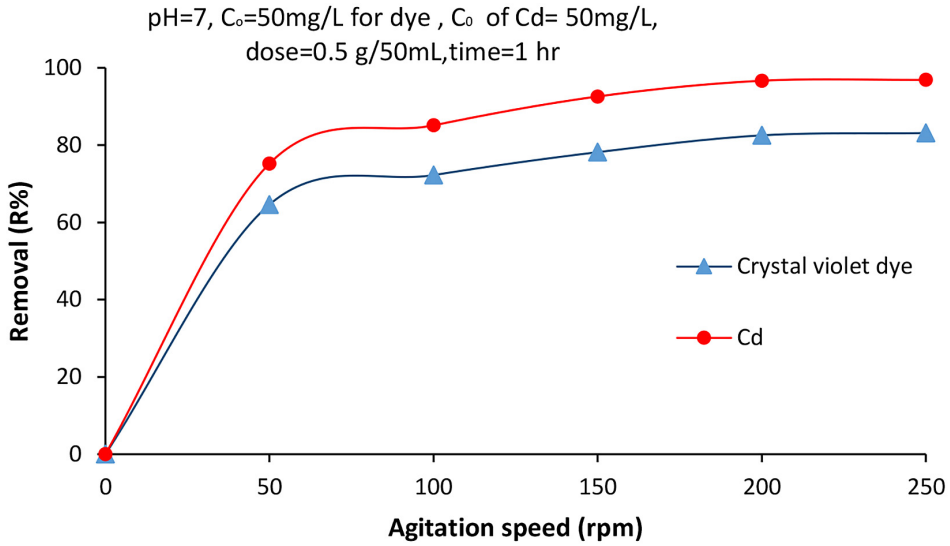

Figure 4. Effect of agitation speed on the manufactured composite adsorbent behavior used for removing dye and cadmium from contaminated aqueous solution.

from the aqueous solution. Results revealed that the maximum removal efficiency of the dye was (98.0128%) at pH of 12. Adsorption of dye ions increases at basic condition at pH 12, thus as a result of strong interactions that formed between the positively charged dye molecules and the negatively charged adsorbent surface at high pH values. In contrast, hydrogen ions competed with the positively charged dye molecules in low pH solutions, resulting in a reduced percentage of dye removal [40]. When pH is lower than 12, there will repulsion between crystal violet dye and composite, hence dye adsorption is decreased. The plot 5 demonstrates that the greatest removal efficiency (99.56%) of Cd, at pH of 6. At acidic pH, the excessive H^+ ions compete with the Cd^{+2} ions for sites of adsorption and reduce the efficiency of removal. A gradual reduction in the removal of metal ions was observed at pH of higher values (pH > 6). At higher pH values, negative charge sites increase on the surface of the adsorbent that generates an electrostatic attraction force between the metal ion and the adsorbent [46]. When the pH of an aqueous solution rises over 6, it causes a precipitation of hydroxide ions, which in consequence leads cadmium ions to precipitate [47].

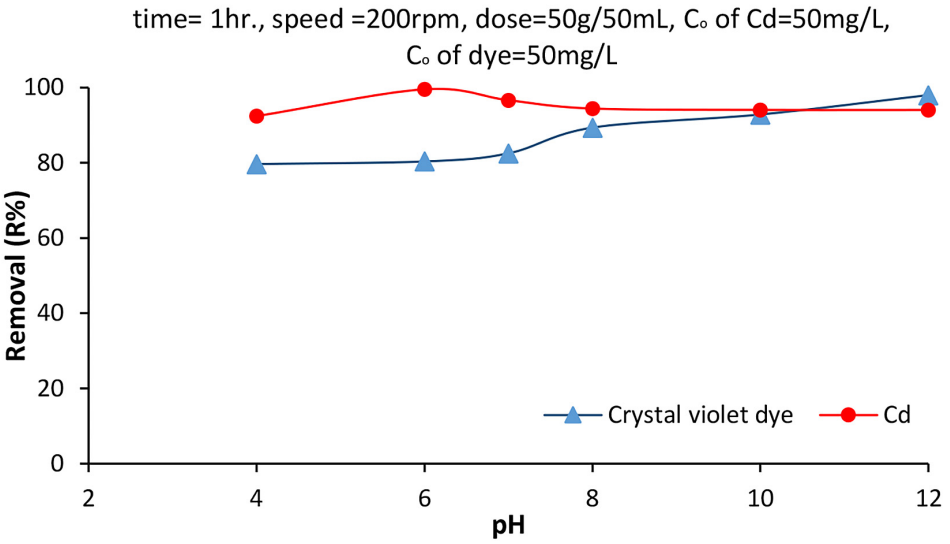

Figure 5. Effect of initial pH on the manufactured adsorbent composite behavior used for removing dye and cadmium from contaminated aqueous solution

Influence of composite dosage

The effect of the composite mass on the crystal violet dye and Cd sorption was examined separately in the range 0.2 to 1.0 g per 50 mL of contaminated solution to determine the optimum dose. On the basis of Figure 6, the efficacy of TC removal increases with the higher amount composite. This could be clarified through the fact that when the composite dosage increase, so the number of effective sites and areas increase [46]. The removal effectiveness of crystal violet dye ranged from 95.531% at 0.2 g to 99.311% at 1 g of adsorbent at pH 12, 50 mg/L, 1 hour, and 200 rpm. The removal effectiveness ranged from 98.8% at 0.2 g to 99.7296% at 1 g of sorbent mass for cadmium at pH of 6, 50 mg/L, 1 hr, and 200 rpm. An increase in dye removal is observed as the dosages are increased as a result of the increased availability of the active sites and adsorbent surface area. Additionally, the capacity of adsorption decreases with increasing dosage because the adsorbate to adsorbent ratio decreases. The adsorption decreases at lower concentrations due to the rapid superficial sorption onto the adsorbent surface [48].

Sorption isotherm

At the end of the sorption process, isotherms show that there is an equilibrium condition amongst the amounts of contaminants molecules on the composite and those amounts in water. The main sorbent parameters that need to be calculated using isotherm models are the maximum capacity of sorption and the intensity distribution of polluting molecules. Table 1 reports the estimated constants from the nonlinear Freundlich and Langmuir models that are enabled by the "Solver" tool in Microsoft Excel 2016 option and used to fit sorption data over composite. On the basis of the highest R^2 and lowest SSE, the Langmuir model was able to effectively reflect the crystal violet dye sorption onto the composite. According to Freundlich, the largest R^2 and lowest SSE determined the ability of the composite to reflect cadmium sorption. The concordance between the sorption isotherm and experimental data is shown in Figure 7 (A and B). Composites are effective in eliminating target pollutants, since cadmium has a maximum adsorption capacity of 48.5052 mg/g and crystal violet dye has a capacity of 40.9682 mg/g.

Sorption kinetics

In this work, the Solver Tool in Microsoft Excel 2016 was used to fit the kinetic results for the change in sorbed target pollutants against experimental time applying non-linear regression Equations 5 and 6. Table 2 shows those constants used in the fitting process for the kinetic models. To determine the level of agreement between the given models and experimental data, the sum of squared errors (SSE) and determination coefficient (R^2) should be computed. These values presented in Figure 8 (A and B) and Table 2. The pseudo-second-order model is more plausible for describing the sorption of crystal violet dye and cadmium onto the generated composite. Thus, it may be argued that chemical forces play a considerable part in the elimination of dissolved contaminants. K_1 and K_2 are used to represent the rate at which the equilibrium of adsorption is accomplished.

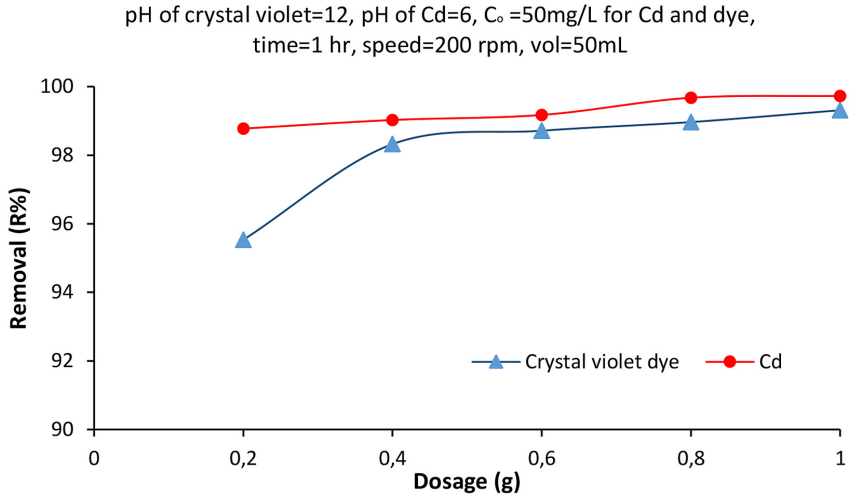

Figure 6. Effect of dosage on the manufactured composite adsorbent behavior used for removing dye and cadmium from contaminated aqueous solution

Table 1. Isotherm model constants for the sorption of contaminants onto the composite

Models	Parameters	Crystal violet	Cadmium (Cd)
Langmuir	q_{max}(mg/g)	40.9682	48.5052
	b(L/mg)	0.1854	0.3783
	R^2	0.9882	0.8586
	SEE	0.7084	12.9819
Freundlich	Kf(mg/g)(L/mg)^(1/n)	6.2024	20.0343
	n	1.210	0.7189
	R^2	0.9844	0.8947
	SEE	0.9232	8.5149

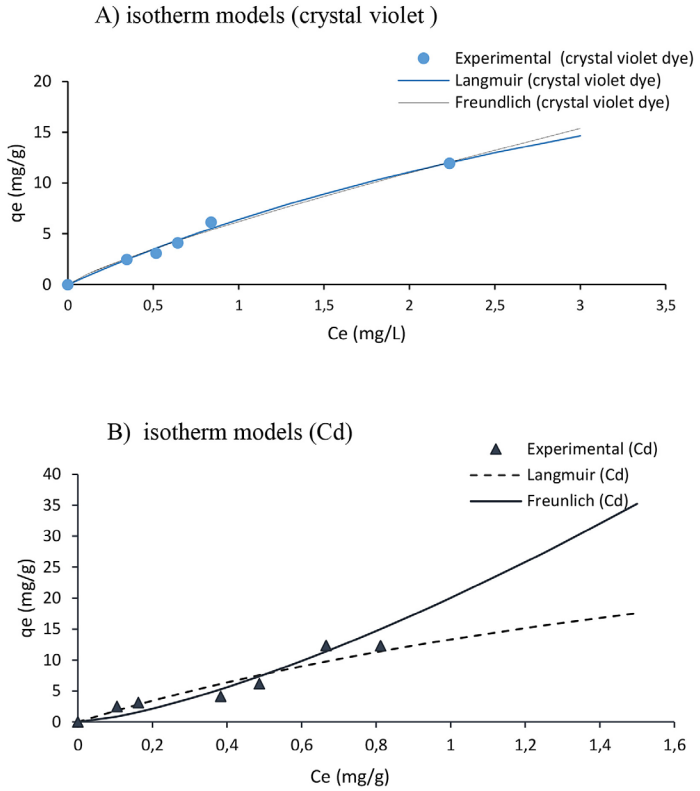

Figure 7. Sorption isotherm models for, A) crystal violet dye, B) cadmium (Cd)

Characterizations of the composite

The X-ray Diffraction (XRD) was exploited for the characterization of the crystal structure of the synthesis composite. The XRD investigation was utilized to ascertain the diffraction patterns associated with the synthesized composite, with 2Θ ranging from 10° to 80°. Figure 9 depicts the XRD profile of the crystalline composition of the composite. The sharp and broad peaks indicate a mixture of crystalline and amorphous zones of composite. A multitude of diffraction reflections (29.378, 34.766, 42.375, 52.963, 56.440, 62.002, 70.517, and 73.5119) were observed, as depicted in Figure 9. These reflections illustrate the active spots in the composite that have the ability to eliminate crystal violet and Cd from an aqueous solution. Figure 10 displays the FTIR spectra (400–4000 cm^{-1}) of the composite before and after the sorption of crystal violet dye and Cd. The spectra consider the main functional groups that enhance the adsorption of pollutants at peaks (3425.577, 3664.75, 1620.205, 547.837, 887.255, 948.477, 1110.998, 1226.727, 1404.178, 447.49, 393.478, and 2368.586) cm^{-1}. Peaks at 3425.577 and 3664.75 cm^{-1} correspond to (-OH) group. The 1620.205 cm^{-1} peaks correspond to (O-H). Peaks 547.837, 447.49, and 887.255 correspond to Fe-O, Mn-O, and Al-O respectively [49–52]. Peaks of 1110.998 and 1404.178 correspond to (C-H) and (C = O), respectively. Directly after adsorption, the

Table 2. Kinetics model constants for the sorption of contaminants onto the composite

Model	Parameters	Crystal violet dye	Cadmium (Cd)
Pseudo-first order	qe (mg/g)	4.9899	4.8432
	K1 (min^{-1})	0.950	0.9899
	R2	0.7798	0.9188
	SEE	6.0811	12.2923
Pseudo-second order	qe (mg/g)	5.1901	5.2297
	K2 (min^{-1})	0.7522	0.7334
	R2	0.8615	0.9620
	SEE	1.3382	1.9860

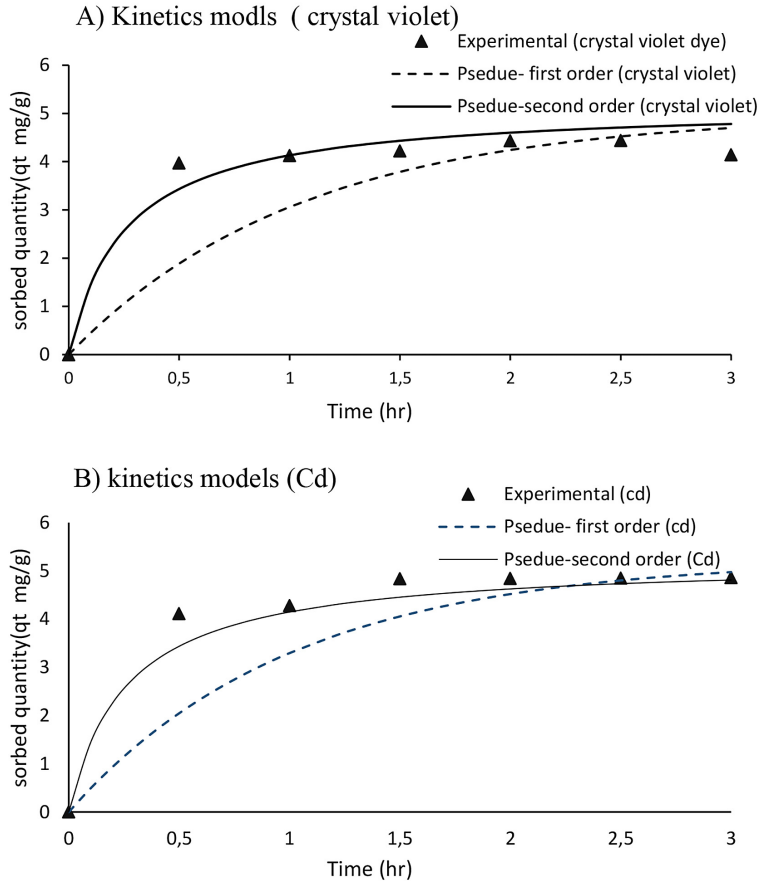

Figure 8. Kinetics models for, A) crystal violet dye, B) cadmium (Cd)

composites (OH) vibrations changed and shifted, indicating the formation of hydrogen bonds. Additionally, FTIR study revealed that the functional groups like (-OH), and (-C = O), were beneficial in crystal violet dye adsorption [53]. The donation of lone-pair electrons from O to Cd^{2+} after cadmium adsorption caused a shift in the binding energies of (-C = O) and (-OH) to low values, resulting in a reduction in electron cloud density of O [41]. The morphological properties of the produced composite may be described using scanning electron microscopy (SEM) graphs, as depicted in Figure 11 (a, b, and c), both before and after treatment with crystal violet and Cd. Significant morphological alterations can be observed in the composite material subsequent to the elimination of contaminants, in comparison with the sorbent material before to the process of sorption. Utilization of EDS graphs enables the characterization of the extent of alteration observed in the elemental proportions of the composite composition, extending beyond the sorption process depicted in Figure 12 (a, b, and c) and Table 3.

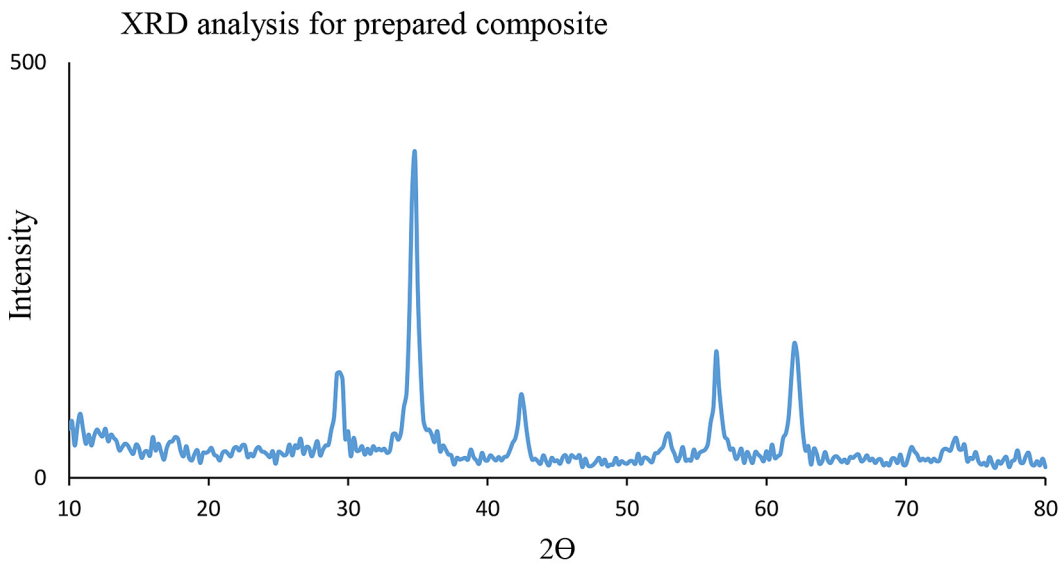

Figure 9. XRD analysis for composite adsorbent

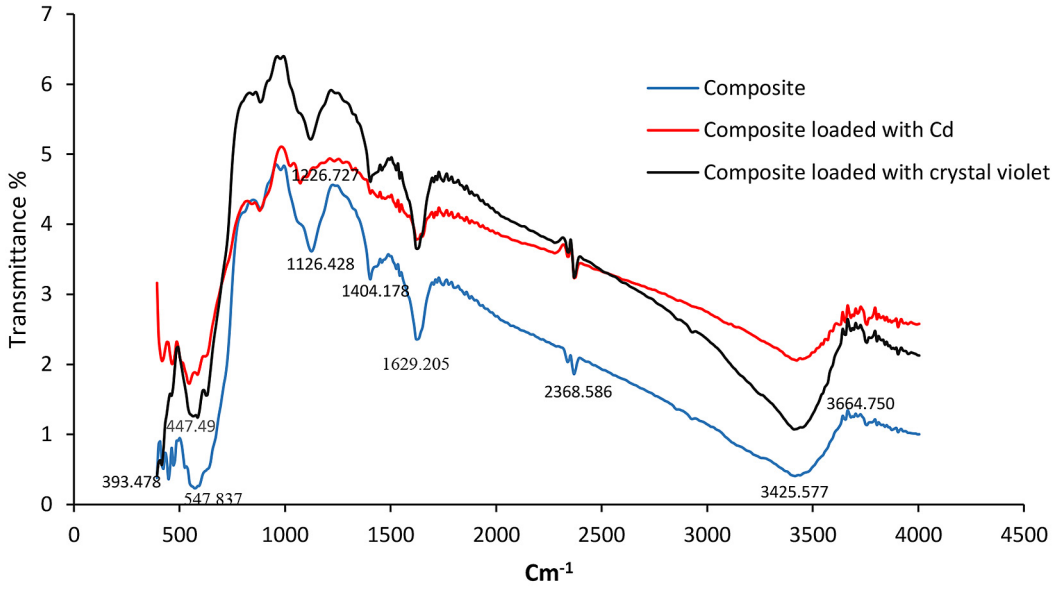

Figure 10. FTIR analysis for composite before and after interaction with dye and Cd

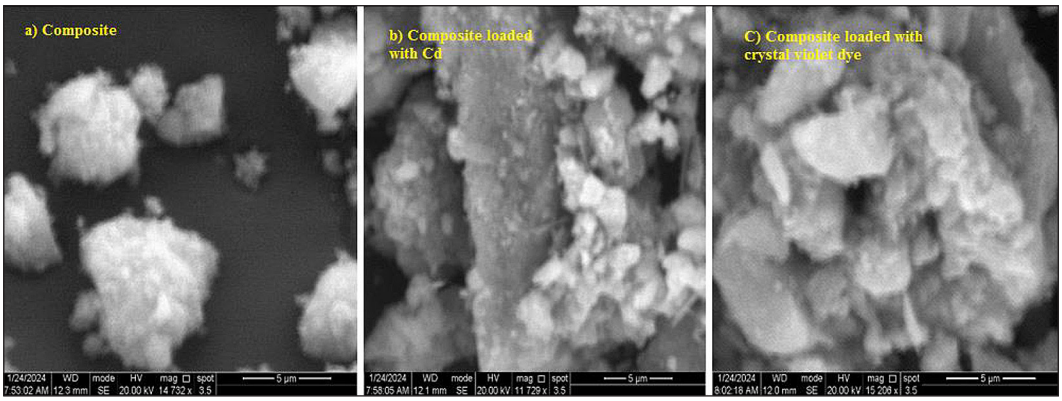

Figure 11. SEM graph, a) composite, b) composite loaded with Cd, c) composite loaded with crystal violet dye

Table 3. elemental composition of produced composite before and after sorption for target contaminants

Element %	Composite	Composite loaded with Cd	Composite loaded with crystal violet
Fe	38.211	20.3	6.44
O	34.242	30.740	16.50
Mn	13.137	12.300	11.44
Al	12.76	11.58	12.103
C	–	–	50.222
Cd	–	24.65	–
Cl	1.65	0.430	3.215
N	–	–	0.08

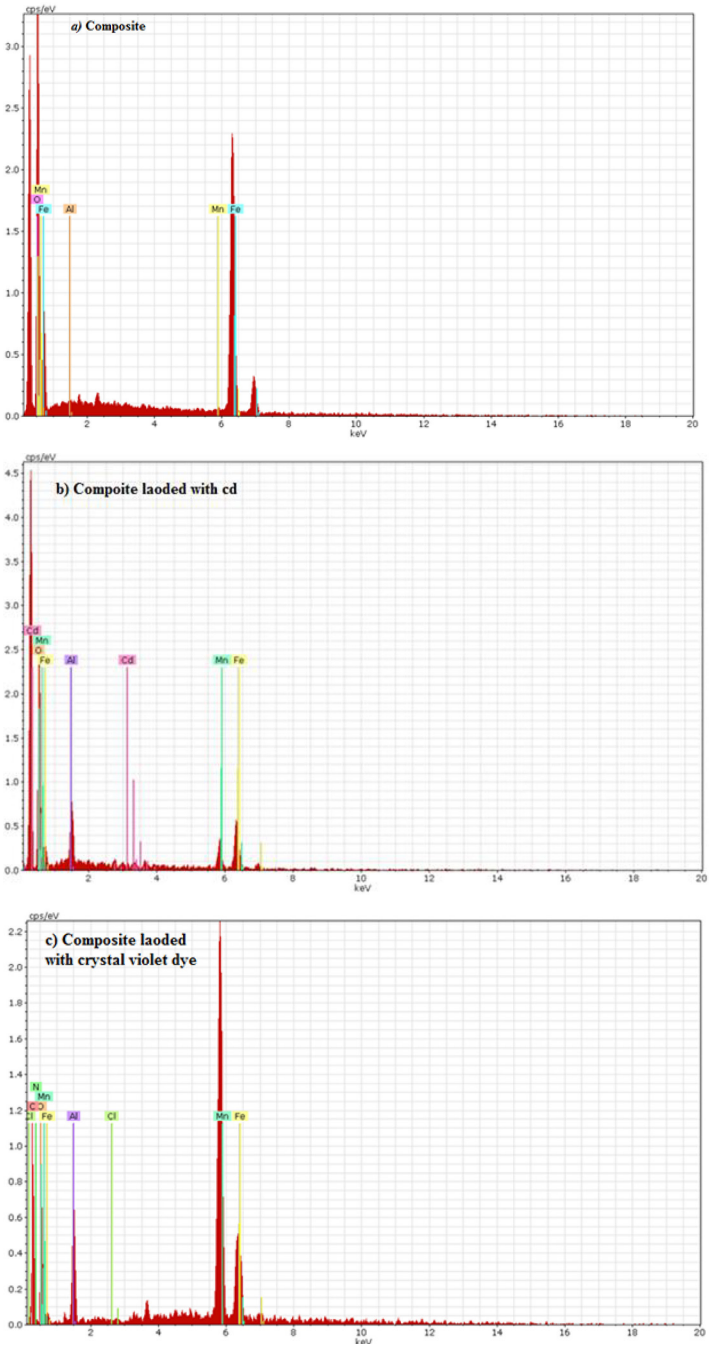

Figure 12. EDS analysis, a) composite, b) composite loaded with Cd, c) composite loaded with crystal violet dye

Table 4. Assessment of the prepared composite adsorption capacity to extract crystal violet dye (CV) from the aqueous solution in comparison to other adsorbents

Adsorbents	Qe (mg/g)	Contact time (h)	C_o (mg/l)	pH	Ref
Fe_3O_4 – coated biochar	349.4	4	400	6	[54]
ACL/Fe_3O_4	35.3	1	10	9	[53]
Poly(Acrylamide-co-Maleic Acid)/Montmorillonite Nanocomposite	23.8	3	100	7	[55]
MNP@PAAA-FA	25.1	3	1	7	[56]
Coconut husk	0.728	1	50	12	[40]
Bentonite – alginate composite	601.93	1	300	8	[48]
(Fe_3O_4@MnO_2@Al_2O_3)	40.968	1	50	12	this study

Table 5. Assessment of the prepared composite adsorption capacity to extract cadmium from the aqueous solution in comparison to other adsorbents.

Adsorbents	Qe (mg/g)	Contact time (h)	C_o (mg/l)	pH	Ref
Fe_3O_4@PDA	21.58	2	20	7	[41]
Bio-nanocomposite of Fe_3O_4 – Actinomucor sp.	29.49	2	400	7	[47]
NPCLA	25.253	1	20.7	6.3	[57]
Cs-Fe_3O_4 - B600	64.31	-	100	8	[58]
BC@MnO_2	33.5	-	-	2	[16]
Recycled lignocelluloses (almond)	78.74	0.75	100	6	[59]
(Fe_3O_4@MnO_2@Al_2O_3)	48.505	1	50	6	This study

COMPARISON WITH PREVIOUS STUDIES

The capacity of adsorption corresponding to various adsorbents can vary according to factors such as the contaminant type, adsorption modification, operating conditions, and the primary source of the adsorbent. Developing adsorbents with high capacity of adsorption and inexpensive economic cost is an evolving area of intense research [53]. For the reasons stated above, this study compared the adsorption capability of the produced composite to that of other synthetic and natural adsorbents utilized in the CV dye and Cd adsorption process; Tables 4 and 5 presented the comparison between the prepared composite and adsorbent in literature for removal of CV and Cd, respectively.

CONCLUSIONS

The present study produced a unique composite adsorbent via coprecipitation method from iron, manganese and aluminum oxides that efficiently removed crystal violet dye and cadmium. The outcomes pointed that the removal efficacies were 99.311% and 99.7296% for crystal violet dye and cadmium, respectively. The outcomes demonstrated that the Langmuir model could accurately depict the sorption of crystal violet dye onto the composite. On the basis of Freundlich, the capacity of the composite to reflect cadmium sorption was determined. The pseudo-second-order model is a more realistic way to explain how cadmium and crystal violet dye sorb onto the composite. The results showed that the prepared adsorbent is effective in removing crystal violet and cadmium, with highest adsorption capacities of 40.9682 mg/g and 48.5052 mg/g. The (Fe_3O_4@MnO_2@Al_2O_3) composite had promising adsorption capabilities for the removal of dye and heavy metals from simulated industrial effluent. The most important recommendation for this study is to determine if the prepared composite can be used in Fixed-bed column experiments in addition to batch experiments. This will allow examining how different parameters like flow rate and bed height, affect the ability of the composite to remove Cd and crystal violet dye from the aqueous

solution. Using the prepared composite for the removal of additional pollutants, such as antibiotics and petroleum pollution can be considered.

REFERENCES

1. Mokif L.A., Faisal A.A.H. 2023. Funnel and Gate Permeable Reactive Barrier Permeable Reactive Barrier Configuration for Contaminated Groundwater Remediation – Designing, Installation, and Modeling : A Review, 2415–33.
2. Mokif L.A. 2015. Research Article Evaluation of Treated Water at Three Adjacent Water Treatment Stations in Al-Hilla City, Iraq by Using CCME Water Quality Index, Res. J. Appl. Sci. Eng. Technol. 10, 1343–1346.
3. Mokif L.A. 2020. New Natural Coagulant for Biochemical Oxygen Demand (BOD) Removal from Domestic Wastewater, 24, 66–68.
4. Rafaqat S., Ali N., Torres C., Rittmann B. 2022. Recent progress in treatment of dyes wastewater using microbial-electro-Fenton technology, RSC Adv. 12, 17104–17137.
5. Dutta S., Gupta B., Srivastava S.K., Gupta A.K. 2021. Materials Advances Recent advances on the removal of dyes from wastewater using various adsorbents : a critical, 4497–4531. https://doi.org/10.1039/d1ma00354b
6. Mokif L.A., Abdulhusain N.A. 2022. A Low Cost Material for Treatment Wastewater Contained Petroleum Pollution, in: IOP Conf. Ser. Earth Environ. Sci., IOP Publishing, 12014.
7. Liu Q. 2020. Pollution and treatment of dye wastewater, in: IOP Conf. Ser. Earth Environ. Sci., IOP Publishing, 52001.
8. Aragaw T.A., Bogale F.M. 2021. Biomass-Based Adsorbents for Removal of Dyes From Wastewater : a review, 9. https://doi.org/10.3389/fenvs.2021.764958
9. Al-Tohamy R., Ali S.S., Li F., Okasha K.M., Mahmoud Y.A.-G., Elsamahy T., Jiao H., Fu Y., Sun J. 2022. A critical review on the treatment of dye-containing wastewater: Ecotoxicological and health concerns of textile dyes and possible remediation approaches for environmental safety, Ecotoxicol. Environ. Saf. 231, 113160.
10. Kandisa R.V., Kv N.S., Shaik K.B. 2016. Gopinath R. Bioremediation & Biodegradation Dye Removal by Adsorption : A Review, 7. https://doi.org/10.4172/2155-6199.1000371
11. Zaim M., Zaimee A., Sarjadi M.S. 2021. Heavy Metals Removal from Water by Efficient Adsorbents.
12. Abdulhusain N.A., Mokif L.A. 2023. The Removal Performance of Bio-Sorption on Sunflower Seed Husk for Copper and Lead Ions from Aqueous Solutions, 24, 110–117.
13. Sankhla M.S., Kumari M., Nandan M., Kumar R., Agrawal P. 2016. Heavy metals contamination in water and their hazardous effect on human health-a review, Int. J. Curr. Microbiol. App. Sci. 5, 759–766.
14. Zhu F., Zheng Y.-M., Zhang B.-G., Dai Y.-R. 2021. A critical review on the electrospun nanofibrous membranes for the adsorption of heavy metals in water treatment, J. Hazard. Mater. 401, 123608.
15. Renu M., Agarwal K. Singh. 2017. Heavy metal removal from wastewater using various adsorbents: a review, J. Water Reuse Desalin. 7, 387–419.
16. Zhang H., Xu F., Xue J., Chen S., Wang J. 2020. Enhanced removal of heavy metal ions from aqueous solution using manganese dioxide-loaded biochar : Behavior and mechanism, Sci. Rep. 1–13. https://doi.org/10.1038/s41598-020-63000-z
17. Ruan W., Hu J., Qi J., Hou Y., Zhou C., Wei X. 2019. Removal of dyes from nanomaterials : A review wastewater by, 10, 9–20. https://doi.org/10.5185/amlett.2019.2148
18. Gopalakrishnan A., Krishnan R., Thangavel S., Venugopal G., Kim S.-J. 2015. Removal of heavy metal ions from pharma-effluents using graphene-oxide nanosorbents and study of their adsorption kinetics, J. Ind. Eng. Chem. 30, 14–19.
19. Al-alawy A.F., Al-abodi E.E., Kadhim R.M. 2018. Journal of Engineering, 24, 60–72.
20. Fizikokimia S., Magnetit N., Sebagai F.O., Pepejal P., Homogen M. 2018. Synthesis and physicochemical properties of magnetite nanoparticles (Fe_3O_4) as potential solid support for homogeneous catalysts, 22, 768–774.
21. Wei Y., Han B., Hu X., Lin Y. 2012. Procedia Engineering Synthesis of Fe_3O_4 nanoparticles and their magnetic properties, 0–5. https://doi.org/10.1016/j.proeng.2011.12.498
22. Webster T.J., Kuča K. 2021. Green Synthesis of Fe_3O_4 Nanoparticles Stabilized by a Garcinia mangostana Fruit Peel Extract for Hyperthermia and Anticancer Activities, 2515–2532.
23. Suman H., Sangal V.K., Chen C., Cai F. 2019. Synthesis of Fe_3O_4 nanoparticles for colour removal of printing ink solution Synthesis of Fe_3O_4 nanoparticles for colour removal of printing ink solution. https://doi.org/10.1088/1742-6596/1245/1/012040
24. Abdulkareem L., Ayad M. 2023. Laboratory Studies into Tetracycline Removal from Aqueous Solutions by Beads of Calcium - Iron Oxide Nanoparticles, Water, Air, Soil Pollut. https://doi.org/10.1007/s11270-023-06585-1
25. Iskandar F., Asbahri A., Dwinanto E., Abdullah M. 2015. Synthesis of Fe_3O_4 Nanoparticles Using the Co-Precipitation Method and Its Development into Nanofluids as a Catalyst in Aquathermolysis

Reactions, 1112, 205–208. https://doi.org/10.4028/www.scientific.net/AMR.1112.205

26. Ganapathe L.S., Kazmi J. 2022. Molarity Effects of Fe and NaOH on Synthesis and Characterisation of Magnetite (Fe_3O_4) Nanoparticles for Potential Application in Magnetic Hyperthermia Therapy.
27. Darminto D., Baqiya M., Cahyono Y., Triwikantoro T. 2011. Preparing Fe_3O_4 Nanoparticles from Fe_2 + Ions Source by Co - precipitation Process in Various pH Preparing Fe_3O_4 Nanoparticles from Fe_2 + Ions Source by Coprecipitation Process in Various pH View online : http://dx.doi.org/10.1063/1.3667264 View Table of Contents : http://scitation.aip.org/content/aip/proceeding/aipcp/1415?ver=pdfcov Published by the AIP Publishing, 4–9. https://doi.org/10.1063/1.3667264
28. Mohammadi H., Nekobahr E., Akhtari J., Saeedi M., Akbari J. 2021. Synthesis and characterization of magnetite nanoparticles by co-precipitation method coated with biocompatible compounds and evaluation of in-vitro cytotoxicity, Toxicol. Reports. 8, 331–336. https://doi.org/10.1016/j.toxrep.2021.01.012
29. Ba-abbad M.M., Benamour A., Ewis D., Mohammad A.W. 2022. Synthesis of Fe_3O_4 Nanoparticles with Different Shapes Through a Co-Precipitation Method and Their Application, JOM. 74, 3531–3539. https://doi.org/10.1007/s11837-022-05380-3
30. Hariani P.L., Faizal M., Setiabudidaya D. 2013. Synthesis and Properties of Fe_3O_4 Nanoparticles by Co-precipitation Method to Removal Procion Dye, 4. https://doi.org/10.7763/IJESD.2013.V4.366
31. Prabowo B., Khairunnisa T., Bayu A., Nandiyanto D. 2018. Economic Perspective in the Production of Magnetite (Fe_3O_4) Nanoparticles by Co-precipitation Method, 2, 1–4.
32. Rahmat M., Rehman A., Rahmat S., Nawaz H. 2019. Highly efficient removal of crystal violet dye from water by MnO_2 based nanofibrous mesh / photocatalytic process, Integr. Med. Res. 8, 5149–5159. https://doi.org/10.1016/j.jmrt.2019.08.038
33. Abbas R.F., Hami H.K., Mahdi N.I., Waheb A.A. 2020. Removal of Eriochrome Black T Dye by Using Al_2O_3 Nanoparticles : Central Composite Design, Isotherm and Error Analysis, Iran. J. Sci. Technol. Trans. A Sci. 6. https://doi.org/10.1007/s40995-020-00911-6
34. Lai S.O., Chong K.C., Kerk Z.W., Ooi B.S., Lau W.J. 2017. Fabrication of PES/MnO mixed matrix membranes for cadmium removal, Malaysian J Anal Sci. 21, 381–390.
35. Wang Y., Gong S., Li Y., Li Z., Fu J. 2020. Adsorptive removal of tetracycline by sustainable ceramsite substrate from bentonite/red mud/pine sawdust, Sci. Rep. 10, 1–18. https://doi.org/10.1038/s41598-020-59850-2
36. Hassan W., Faisal A., Abed E., Al-Ansari N., Saleh B. 2021. New composite sorbent for removal of sulfate ions from simulated and real groundwater in the batch and continuous tests, Molecules. 26. https://doi.org/10.3390/molecules26144356
37. Lagergren S. 1989. About the theory of so-called adsorption of soluble substances, K. Seventeen Hand. 24, 1–39.
38. Ho Y.S., McKay G. 1999. Pseudo-second order model for sorption processes, Process Biochem. 34, 451–465.
39. Mokif L.A., Faisal A.A.H. 2023. Manufacturing of cost-effective sorbent from by-product materials for treating real and simulated groundwater contaminated with antibiotics, 30105, 1–14. https://doi.org/10.5004/dwt.2023.30105
40. Sajid M., Javed T., Areej I., Nouman M. 2022. Sequestration of crystal violet dye from wastewater using low-cost coconut husk as a potential adsorbent, 85, 2295–2317. https://doi.org/10.2166/wst.2022.124
41. Lei T., Li S., Jiang F., Ren Z., Wang L., Yang X., Tang L., Wang S. 2019. Adsorption of Cadmium Ions from an Aqueous Solution on a Highly Stable Dopamine-Modified Magnetic Nano- Adsorbent.
42. Bassam R., El Hallaoui A., El Alouani M., Jabrane M., Hassan E., Khattabi E., Tridane M., Belaaouad S. 2021. Studies on the Removal of Cadmium Toxic Metal Ions by Natural Clays from Aqueous Solution by Adsorption Process.
43. Murithi G., Onindo C.O., Wambu E.W., Muthakia G.K. 2014. Com Removal of Cadmium (II) Ions from Water by Adsorption using Water Hyacinth (Eichhornia crassipes) Biomass, 93613–3631.
44. Sukla K., Kumar U. 2021. South African Journal of Chemical Engineering Adsorption of brilliant green dye from aqueous solution onto chemically modified areca nut husk, South African J. Chem. Eng. 35, 33–43. https://doi.org/10.1016/j.sajce.2020.11.001
45. Valizadeh K., Bateni A., Sojoodi N., Ataabadi M.R., Behroozi A.H., Maleki A., You Z. 2022. Magnetized inulin byas a bio-nano adsorbent for treating water contaminated with methyl orange and crystal violet dyes, Sci. Rep. 1–13. https://doi.org/10.1038/s41598-022-26652-7
46. Dehvari M., Jamshidi B., Jorfi S., Pourfadakari S. 2021. Cadmium removal from aqueous solution using cellulose nanofibers obtained from waste sugarcane bagasse (SCB): isotherm, kinetic, and thermodynamic studies, 221, 218–228. https://doi.org/10.5004/dwt.2021.27060
47. Masoudi R., Moghimi H., Azin E., Taheri R.A. 2018. Adsorption of cadmium from aqueous solutions by novel Fe_3O_4-newly isolated Actinomucor sp. bionanoadsorbent: functional group study, Artif. Cells, Nanomedicine, Biotechnol. 46, 1092–1101.

48. Fabryanty R., Valencia C., Edi F., Nyoo J. 2017. Journal of Environmental Chemical Engineering Removal of crystal violet dye by adsorption using bentonite – alginate composite, 5, 5677–5687. https://doi.org/10.1016/j.jece.2017.10.057
49. Ghelani D., Faisal S. 2022. Synthesis and characterization of Aluminium Oxide nanoparticles, Authorea Prepr.
50. Ali O.I., Azzam A.B. 2023. Functional Ag - EDTA - modified MnO_2 nanocoral reef for rapid removal of hazardous copper from wastewater, Environ. Sci. Pollut. Res. 30, 123751–123769. https://doi.org/10.1007/s11356-023-30805-0
51. Divya P. 2019. Synthesis and Characterization of MnO_2 Nano particles Prepared by Hydrothermal Processing, 2–9.
52. Mokif L.A., Faisal A.A.H. 2023. Manufacturing of cost-effective sorbent from by-product materials for treating real and simulated groundwater contaminated with antibiotics, Desalin. WATER Treat. 314, 35–48.
53. Foroutan R., Peighambardoust S.J., Peighambardoust S.H., Pateiro M., Lorenzo J.M. 2021. Adsorption of Crystal Violet Dye Using Activated Carbon of Lemon Wood and Activated Carbon / Fe_3O_4 Magnetic, 1–19.
54. Sun P., Hui C., Khan R.A., Du J., Zhang Q., Zhao Y. 2015. Efficient removal of crystal violet using Fe_3O_4 -coated biochar : the role of the Fe_3O_4 nanoparticles and modeling study their adsorption behavior, Nat. Publ. Gr. 1–12. https://doi.org/10.1038/srep12638
55. Aref L., Navarchian A.H., Dadkhah D. 2016. Adsorption of Crystal Violet Dye from Aqueous Solution by Poly (Acrylamide- co -Maleic Acid)/ Montmorillonite Nanocomposite, J. Polym. Environ. 9–11. https://doi.org/10.1007/s10924-016-0842-z
56. Ganea I., Nan A., Baciu C. 2021. Effective Removal of Crystal Violet Dye Using Neoteric Magnetic Nanostructures Based on Functionalized Poly (Benzofuran- co -Arylacetic Acid): Investigation of the Adsorption Behaviour and Reusability.
57. Pourjaafar M., Askari A., Salehi A., Abadi S., Anvaripour B., Nemati A., Rahimi S.A. 2023. Removal of cadmium from aqueous solution using nano Prosopis cineraria leaf ash (NPCLA), Kerman Univ. Med. Sci. 10, 225–233. https://doi.org/10.34172/EHEM.2023.25
58. Char F.B., Yang W., Luo W., Sun T., Xu Y., Sun Y. 2022. Adsorption Performance of Cd (II) by Chitosan- Fe_3O_4 -Modified.
59. Kayranli B. 2022. Cadmium removal mechanisms from aqueous solution by using recycled lignocelluloses, Alexandria Eng. J. 61, 443–457. https://doi.org/10.1016/j.aej.2021.06.036